Journal of Materials Science: Materials in Electronics (2018) 29:20517–20521
https://doi.org/10.1007/s10854-018-0188-5

Enhanced long afterglow of $SrAl_2Si_2O_8:Eu^{2+}$ by codoping Dy^{3+}

Zhen Wei[1,2] · Weixi Mao[1] · Kehui Zhang[3] · Ye Tian[1,2]

Received: 18 August 2018 / Accepted: 6 October 2018 / Published online: 11 October 2018

Abstract
Eu^{2+}/Dy^{3+} doped $SrAl_2Si_2O_8$ phosphors were synthesized by a solid state reaction. The phase and luminescent properties of the synthesized phosphors were investigated by the X-ray powder diffraction, photoluminescence spectra, decay curves and the thermo-luminescence glow curves. The XRD results show that the doped Eu^{2+}/Dy^{3+} has no influence on the phase of $SrAl_2Si_2O_8$. The incorporation of Dy^{3+} could significantly enhance the intensity and prolong the afterglow duration of $SrAl_2Si_2O_8:Eu^{2+}$. The co-doped Dy^{3+} ions act as trap centers and trap the electrons generated during exposure of the phosphor to an excitation source, which induces the longer afterglow comparing with Eu^{2+} singly doped $SrAl_2Si_2O_8$ phosphor.

1 Introduction

Long afterglow phosphors are a special type of luminescent material with persistent luminescence that lasts for several minutes or hours after the removal of the activated light source. It is generally accepted that the persistent luminescence involves luminescence and trap centers in a long afterglow phosphor [1]. Charge carriers are generated by the excitation in the luminescence centers and subsequently trapped in the trap centers. If the traps are deep, the carriers may reside there for an infinite time when no external stimulation is provided. Their de-trapping is thermally activated, which can cause a delay in the spectral emission and result in the persistent luminescence. Long afterglow phosphors have wide applications in various fields, such as displays, lighting devices, traffic signs, emergency signages, textile printing, decorations and watch dials [2]. Since the first report of $SrAl_2O_4:Eu^{2+}$, Dy^{3+} persistent phosphor [3], rare earth ions doped persistent phosphors have continuously gained popularity. Among various materials, alkaline earth metal (Ca, Sr, Ba) aluminates or silicates have attracted great attention because there are relatively wide band gaps. It has been found that they are suitable for persistent luminescence centers of Eu^{2+} and Ce^{3+} [4].

Aluminosilicate compounds have been extensively studied as an important family of host materials for rare earth ions because of their excellently physical and chemical properties, high efficiency and thermal stability [5]. Among various aluminosilicate compounds, (Ca, Sr, Ba)$Al_2Si_2O_8$ have been reported to act as hosts for various rare earth ions [6–12]. Moreover, it has been found that it can show long afterglow properties after the dopant of Eu^{2+} [12]. In this work, we report on the synthesis and long afterglow luminescence of Eu^{2+}/Dy^{3+} doped $SrAl_2Si_2O_8$ phosphors. The role of Dy^{3+} in $SrAl_2Si_2O_8:Eu^{2+}$ phosphor for the extension of luminescence has been investigated.

2 Materials and methods

$SrAl_2Si_2O_8:0.02Eu^{2+}$, $SrAl_2Si_2O_8:0.02Dy^{3+}$ and $SrAl_2Si_2O_8:0.02Eu^{2+}/0.02Dy^{3+}$ phosphors were synthesized by a solid state reaction. $SrCO_3$ (99.5%), α-Al_2O_3 (99.5%), SiO_2 (99.0%), Eu_2O_3 (99.99%) and Dy_2O_3 (99.99%) were used as starting materials. In the synthesis, stoichiometric amounts of raw materials were weighted and mixed thoroughly in an agate mortar by grinding for 60 min. The obtained mixture subsequently was transferred to an alumina crucible and calcined at 1400 °C for 6 h in a muffle furnace. The $SrAl_2Si_2O_8:0.02Dy^{3+}$ was calcined in air, but $SrAl_2Si_2O_8:0.02Eu^{2+}$ and $SrAl_2Si_2O_8:0.02Eu^{2+}/0.02Dy^{3+}$ were calcined under a reducing atmosphere (5% H_2/95%

✉ Ye Tian
tianyehb@sohu.com

[1] College of Science, Hebei North University, Zhangjiakou 075000, China

[2] Engineering Technology Research Center of Population Health Informatization in Hebei Province, Zhangjiakou 075000, China

[3] College of Electrical Engineering, Hebei University of Architecture and Engineering, Zhangjiakou 075000, China

N_2). After that, the products were cooled to room temperature in the furnace, collected and re-grinded for the next measurements.

The X-ray diffraction (XRD) patterns were performed on a Rigaku D/max-RA X-ray diffractometer with Cu Kα radiation (λ = 1.5406 Å) at 40 kV and 30 mA. The data were recorded in a 2θ angle of 10°–55° with a scan speed of 10°/min. The excitation and emission spectra were measured by an Edinburgh Instrument FLS920 spectrophotometer equipped with a 150 W xenon lamp as the excitation source and a grating to select a suitable excitation wavelength with excitation and emission slit widths of 2.5 nm, as well as a scan rate of 600 nm/min. Afterglow decay curves were measured by a PR305 long-lasting luminescence detector after the samples were irradiated by ultraviolet light at 365 nm for 10 min. The thermo-luminescence measurements were carried out in the temperature range of 300–500 K with a heating rate of 1 K/s.

3 Results and discussion

Figure 1 shows the XRD patterns of $SrAl_2Si_2O_8$:0.02Eu^{2+}, $SrAl_2Si_2O_8$:0.02Dy^{3+} and $SrAl_2Si_2O_8$:0.02Eu^{2+}/0.02Dy^{3+} phosphors. All of diffraction peaks are well accordance with the standard data of JCPDs 38-1454, indicating that the doped Eu^{2+}/Dy^{3+} ions have no significant influence on the structure of $SrAl_2Si_2O_8$ host. There are no diffractions peaks corresponding to other materials, suggesting that Eu^{2+}/Dy^{3+} ions have doped into $SrAl_2Si_2O_8$ host entirely. There is only one Sr^{2+} crystallographic site in the monoclinic $SrAl_2Si_2O_8$ unit cell and the Sr^{2+} is bonded to eight oxygen atoms forming an irregular hexahedron, but the Al^{3+} and Si^{4+} connect four O atoms to form three-dimensional $(Al/Si)O_4$ frameworks and creates an infinite net structure by corner-sharking. Due to similar ionic radii of Eu^{2+} (1.25 Å, CN = 8), Dy^{3+} (1.027 Å, CN = 8) and Sr^{2+} (1.26 Å, CN = 8), Eu^{2+} and Dy^{3+} ions substitute the Sr^{2+} sites in the synthesized phosphors.

Figure 2 presents the excitation and emission spectra of $SrAl_2Si_2O_8$:0.02Eu^{2+}. By monitoring the emission at 415 nm, the excitation spectrum of $SrAl_2Si_2O_8$:0.02Eu^{2+} exhibits a strong excitation band with a peak at about 365 nm, which results from the $4f^7 \rightarrow 4f^6$ 5d transitions of Eu^{2+} [13]. Under the excitation at 365 nm, the emission spectrum of $SrAl_2Si_2O_8$:0.02Eu^{2+} shows a strong emission band with a peak at about 415 nm, which originates from the spin-allowed transition from the 5d to the 4f state of Eu^{2+} [4]. Figure 3 gives the excitation and emission spectra of $SrAl_2Si_2O_8$:0.02Dy^{3+}. The excitation spectrum monitored

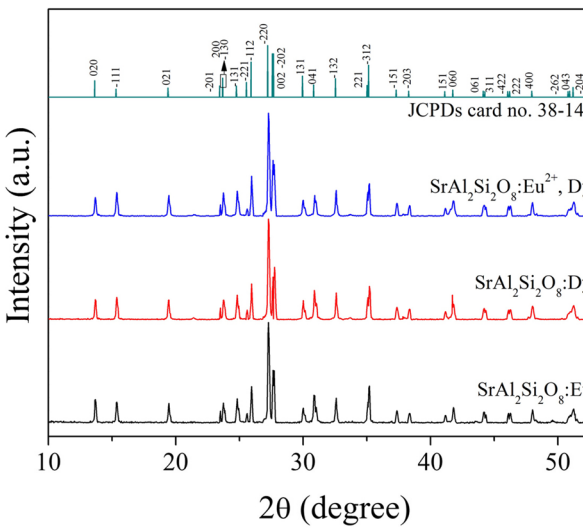

Fig. 1 XRD patterns of $SrAl_2Si_2O_8$:0.02Eu^{2+}, $SrAl_2Si_2O_8$:0.02Dy^{3+} and $SrAl_2Si_2O_8$:0.02Eu^{2+}/0.02Dy^{3+}

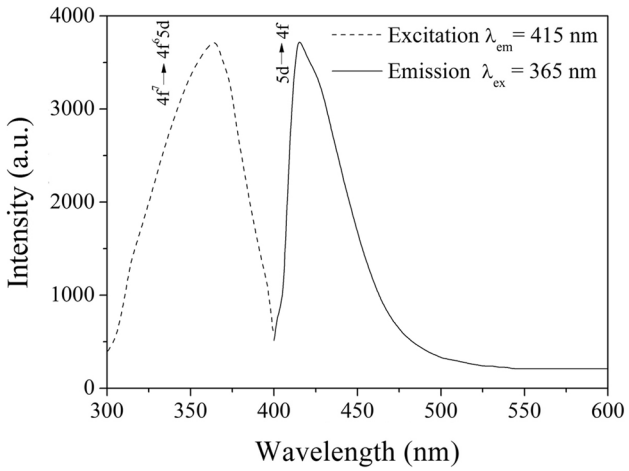

Fig. 2 Excitation and emission spectra of $SrAl_2Si_2O_8$:0.02Eu^{2+}

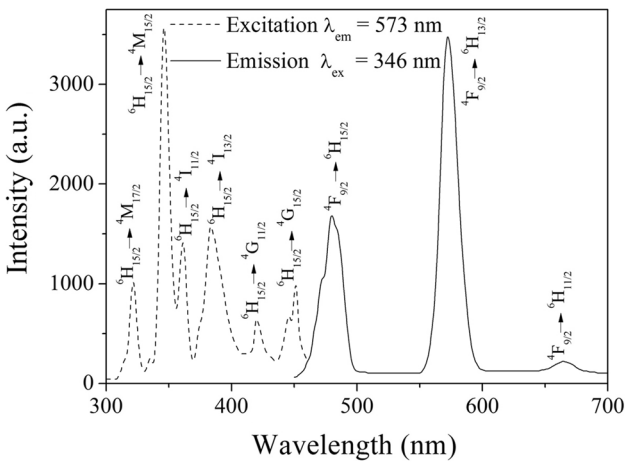

Fig. 3 Excitation and emission spectra of $SrAl_2Si_2O_8$:0.02Dy^{3+}

at 573 nm consists of a series of excitation bands in the range of 300–500 nm with peaks at about 322 nm, 346 nm, 361 nm, 383 nm, 420 nm, 446 nm and 451 nm, which come from the $^6H_{15/2} \rightarrow {}^4M_{17/2}$, $^6H_{15/2} \rightarrow {}^4M_{15/2}$, $^6H_{15/2} \rightarrow {}^4I_{11/2}$, $^6H_{15/2} \rightarrow {}^4I_{13/2}$, $^6H_{15/2} \rightarrow {}^4G_{11/2}$ and $^6H_{15/2} \rightarrow {}^4G_{15/2}$ transitions of Dy^{3+} [14]. Among these excitation bands, the excitation band peaking at 346 nm is much stronger than other excitation bands. Under the excitation at 346 nm, $SrAl_2Si_2O_8$:0.02Dy^{3+} exhibits three emission bands peaking at 480 nm, 573 nm and 664 nm, which originate from the $^4F_{9/2} \rightarrow {}^6H_{15/2}$, $^4F_{9/2} \rightarrow {}^6H_{13/2}$ and $^4F_{9/2} \rightarrow {}^6H_{11/2}$ transitions of Dy^{3+}, respectively [15]. It is known that the yellow emission originating from the $^4F_{9/2} \rightarrow {}^6H_{13/2}$ transition belongs to a hypersensitive (forced dielectric dipole) transition with the selection rule $\Delta J = 2$, which is influenced by the surrounding environment. However, the blue emission corresponding to the $^4F_{9/2} \rightarrow {}^6H_{15/2}$ transition is a magnetic dipole transition, which hardly varies with the crystal field around Dy^{3+} ions. The yellow emission is predominant only when Dy^{3+} ions locate at low-symmetry sites without inversion centers, but the blue emission will be predominant if the ligand-field deviates from inversion symmetry in the host [16]. The stronger yellow emission indicates that Dy^{3+} ions are in the low symmetry sites without inversion. That is consistent with coordination surrounding of Sr^{2+} ions.

Figure 4 exhibits the excitation and emission spectra of $SrAl_2Si_2O_8$:0.02Eu^{2+}/0.02Dy^{3+}. There is only one excitation band peaking at about 365 nm in the excitation spectrum of $SrAl_2Si_2O_8$:0.02Eu^{2+}/0.02Dy^{3+}, which does not show any significant changes from the $SrAl_2Si_2O_8$:0.02Eu^{2+} except for the higher intensity. And this excitation band is also induced by the $4f^7 \rightarrow 4f^6$ 5d transitions of Eu^{2+}. Under the excitation at 365 nm, $SrAl_2Si_2O_8$:0.02Eu^{2+}/0.02Dy^{3+} shows an emission spectrum consisting of a strong emission band with a peak at about 416 nm. The luminescence of $SrAl_2Si_2O_8$:0.02Eu^{2+}/0.02Dy^{3+} tells us that there is no energy transfer between Eu^{2+}/Dy^{3+} ion pairs although the emission spectrum of $SrAl_2Si_2O_8$:0.02Eu^{2+} overlaps with the excitation spectrum of $SrAl_2Si_2O_8$:0.02Dy^{3+}. Figure 5 presents the afterglow decay curves of $SrAl_2Si_2O_8$:0.02Eu^{2+} and $SrAl_2Si_2O_8$:0.02Eu^{2+}/0.02Dy^{3+}. The initial afterglow intensity shows a rapid decay process firstly and then it displays slow decay with lasting decay time. The decay times of $SrAl_2Si_2O_8$:0.02Eu^{2+} and $SrAl_2Si_2O_8$:0.02Eu^{2+}/0.02Dy^{3+} are about 20.6 min and 33.7 min, respectively. It can be seen that the decay time of $SrAl_2Si_2O_8$:0.02Eu^{2+}/0.02Dy^{3+} is longer than that of $SrAl_2Si_2O_8$:0.02Eu^{2+}, which is induced by the hole traps corresponding to the codoped Dy^{3+} ions [12]. The co-doped Dy^{3+} ions act as trap centers and trap the electrons generated during exposure of the phosphor to an excitation source and the afterglow mechanism could be described as producing more traps and stabilizing trapping electrons. On one hand, parts of the divalent alkaline earth cation (Sr^{2+}) were replaced aliovalently by the trivalent rare earth cation (Dy^{3+}) in $SrAl_2Si_2O_8$. In order to keep charge balance, a strontium vacancy (V_{Sr}'') and two Dy_{Sr} sites were generated. This process can be express by the formula of $3Sr_{Sr} \rightarrow 2Dy_{Sr} + V_{Sr}''$ [17]. Therefore, new traps would capture more charge carrying. This result means the concentration of trapped charge will increase. When these carriers were released by thermal agitation at room temperature, $SrAl_2Si_2O_8$:0.02Eu^{2+}/0.02Dy^{3+} can emit a stronger afterglow than before. On the other hand, the optical electronegativity of the Dy^{3+} cation (1.21 eV) is very suitable for stabilizing the captured electrons around traps.

In order to understand the trapping nature of the synthesized phosphors and study the effect of codoped Dy^{3+}

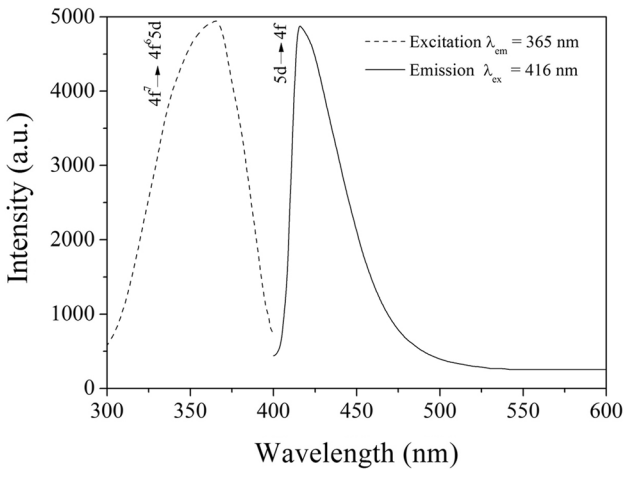

Fig. 4 Excitation and emission spectra of $SrAl_2Si_2O_8$:0.02Eu^{2+}/0.02Dy^{3+}

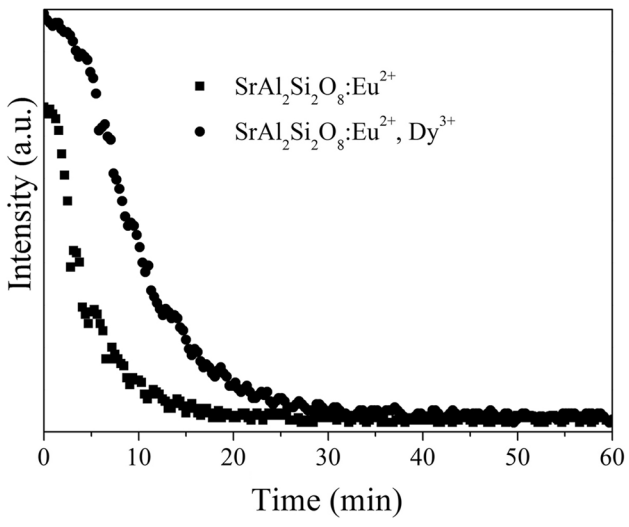

Fig. 5 Afterglow decay curves of $SrAl_2Si_2O_8$:0.02Eu^{2+} and $SrAl_2Si_2O_8$:0.02Eu^{2+}/0.02Dy^{3+}

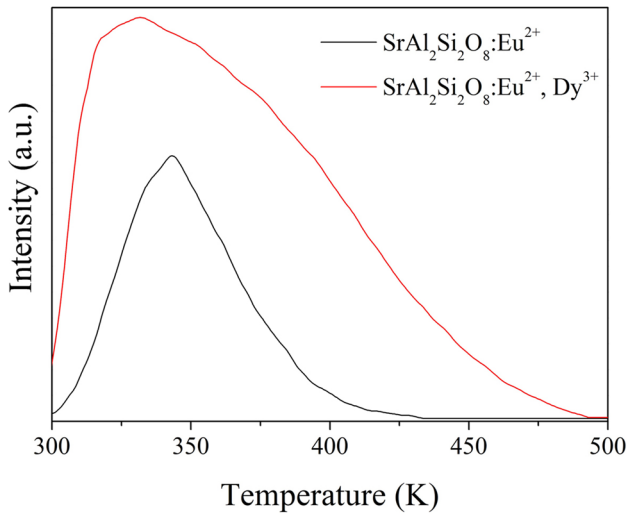

Fig. 6 Thermo-luminescence spectra of $SrAl_2Si_2O_8:0.02Eu^{2+}$ and $SrAl_2Si_2O_8:0.02Eu^{2+}/0.02Dy^{3+}$

ions in $SrAl_2Si_2O_8:Eu^{2+}$ on the persistent luminescence process, thermo-luminescence spectra were measured after stopping 365 nm radiations, as shown in Fig. 6. It can be seen that the emission intensity of thermo-luminescence for $SrAl_2Si_2O_8:0.02Eu^{2+}/0.02Dy^{3+}$ is higher than that of $SrAl_2Si_2O_8:0.02Eu^{2+}$. The higher thermo-luminescence intensity means that there is more traps in $SrAl_2Si_2O_8:0.02Eu^{2+}/0.02Dy^{3+}$. As discussed above, the co-doped Dy^{3+} acts as a trap center and traps the electrons generated during exposure of the phosphor to an excitation source, which induce the higher amount of traps in $SrAl_2Si_2O_8:0.02Eu^{2+}/0.02Dy^{3+}$. Moreover, the profile of thermo-luminescence spectrum for $SrAl_2Si_2O_8:0.02Eu^{2+}/0.02Dy^{3+}$ is wider than that of $SrAl_2Si_2O_8:0.02Eu^{2+}$. The integral area of the thermo-luminescence represents the fact that traps captured the gross amount of charge carriers [4]. The broad thermo-luminescence spectrum covers from 300 to 490 K, which indicates that the traps distribute over a wide range of energies in the bandgap (i.e., traps of various depth were formed).

On the basis of luminescent properties of $SrAl_2Si_2O_8:0.02Eu^{2+}$ and $SrAl_2Si_2O_8:0.02Eu^{2+}/0.02Dy^{3+}$, the possible mechanism of persistent luminescence was speculated. On exposure to an excitation source, an electron of Eu^{2+} ($4f^7$) is promoted to the $4f^65d^1$ band, followed by either direct or phonon-assisted escape of the electron from Eu^{2+} to the host conduction band. The electrons are subsequently captured by shallow traps. During thermal disturbance at room temperature, captured electrons were released from shallow traps and backtracked to the 5d energy levels via a conduction band. Finally, these electrons recombined with emission centers to generate persistent luminescence. Lattice defects close to the bottom of the host conduction band trap the electrons. Huge numbers of electrons are caught by the traps assisted by Dy^{3+} at various depths, highlighting an important role for Dy^{3+} during the long afterglow. After removal of the excitation source, the captured electrons near the host conduction band are released to the conduction band with thermal energy, and their consequent recombination with the emitting Eu^{2+} centers leads to the persistent afterglow.

4 Conclusions

We synthesized Eu^{2+}/Dy^{3+} doped $SrAl_2Si_2O_8$ phosphors through a solid state reaction. Eu^{2+}/Dy^{3+} singly doped $SrAl_2Si_2O_8$ phosphor respectively shows characteristic emission bands of Eu^{2+} or Dy^{3+}, and Eu^{2+}/Dy^{3+} codoped $SrAl_2Si_2O_8$ phosphor only exhibits emission band of Eu^{2+} with higher intensity than that of Eu^{2+} singly doped $SrAl_2Si_2O_8$. Both $SrAl_2Si_2O_8:Eu^{2+}$ and $SrAl_2Si_2O_8:Eu^{2+}/Dy^{3+}$ show long afterglow luminescence. In $SrAl_2Si_2O_8:Eu^{2+}/Dy^{3+}$, Dy^{3+} acts as a trap center and traps the electrons generated during exposure of the phosphor to an excitation source, which induces the longer afterglow comparing with Eu^{2+} singly doped $SrAl_2Si_2O_8$ phosphor. The luminescent properties indicate that $SrAl_2Si_2O_8:Eu^{2+}/Dy^{3+}$ has potential applications in future opto-electronic devices.

Acknowledgements This work is supported by the Basic research Project of Hebei Province (18961031D), the science and technology research project of Hebei's colleges and university (No. BJ2017035), the Science and Technology Research and Development Program of Hebei Province, Zhangjiakou city (17120011D) and the Doctoral Foundation of Hebei North University (12995557).

References

1. P. Chandrakar, R.N. Baghel, D.P. Bisen, B.P. Chandra, Luminescence **31**, 164 (2016)
2. I.P. Sahu, J. Mater. Sci.: Mater. Electron. **26**, 7059 (2015)
3. T. Matsuzawa, Y. Aoki, N. Takeuchi, Y. Murayama, J. Electrochem. Soc. **143**, 2670 (1996)
4. P. Wang, X. Xu, D. Zhou, X. Yu, J. Qiu, Inorg. Chem. **54**, 1690 (2015)
5. B. Yuan, Y. Song, Y. Sheng, K. Zheng, X. Zhou, P. Ma, X. Xu, H. Zou, J. Solid State Chem. **232**, 169 (2015)
6. P. Ma, Y. Song, B. Yuan, Y. Sheng, C. Xu, H. Zou, K. Zheng, Ceram. Int. **43**, 60 (2017)
7. P. Ma, B. Yuan, Y. Sheng, K. Zheng, Y. Wang, C. Xu, H. Zou, Y. Song, J. Alloys Compd. **714**, 627 (2017)
8. X. Zheng, Q. Fei, Z. Mao, Y. Liu, Y. Cai, Q. Lu, H. Tian, D. Wang, J. Rare Earth **29**, 522 (2011)
9. J. Chen, Y. Liu, H. Liu, H. Ding, M. Fang, Z. Huang, Opt. Mater. **42**, 80 (2015)
10. Y. Hua, S. Xu, D. Deng, S. Zhao, H. Wang, L. Huang, Opt. Commun. **284**, 27 (2011)

11. H. Xu, L. Wang, M. Li, W. Ran, Z. Deng, R. Houzong, J. Shi, Phys. Status Solidi A **214**, 1700013 (2017)
12. X. Shi, Y. Wang, Z. Wang, P. Zhang, Z. Hong, X. Fan, G. Qian, Acta Photonica Sin. **37**, 171 (2008)
13. M. Zhao, Z. Zhao, L. Yu, L. Yang, J. Jiang, X. Li, G. Li, J. Mater. Sci.: Mater. Electron. **29**, 1832 (2018)
14. X. Tan, Y. Wang, M. Zhang, J. Photoch. Photobio A **363**, 65 (2018)
15. G. Li, J. Mater. Sci.: Mater. Electron. **27**, 11012 (2016)
16. H. Liu, Z. Guo, J. Lumin. **187**, 181 (2017)
17. G. Chen, F. Wang, J. Yu, H. Zhang, X. Zhang, J. Mol. Struct. **1128**, 1 (2017)